

Dalton Transactions

Accepted Manuscript



This is an *Accepted Manuscript*, which has been through the Royal Society of Chemistry peer review process and has been accepted for publication.

Accepted Manuscripts are published online shortly after acceptance, before technical editing, formatting and proof reading. Using this free service, authors can make their results available to the community, in citable form, before we publish the edited article. We will replace this *Accepted Manuscript* with the edited and formatted *Advance Article* as soon as it is available.

You can find more information about *Accepted Manuscripts* in the [Information for Authors](#).

Please note that technical editing may introduce minor changes to the text and/or graphics, which may alter content. The journal's standard [Terms & Conditions](#) and the [Ethical guidelines](#) still apply. In no event shall the Royal Society of Chemistry be held responsible for any errors or omissions in this *Accepted Manuscript* or any consequences arising from the use of any information it contains.

Quantitative Assessment of the Carbocation/Carbene Character of the Gold-Carbene Bond[†]

Keith M. Azzopardi,^{a,‡} Giovanni Bistoni,^{b,c,‡} Gianluca Ciancaleoni,^{b,*} Francesco Tarantelli,^{b,c}
Daniele Zuccaccia,^{b,d} Leonardo Belpassi^{b,*}

^a Metamaterials Unit, Faculty of Science, University of Malta, Msida, MSD 2080, Malta

^b Istituto di Scienze e Tecnologie Molecolari del CNR (CNR-ISTM), c/o Dipartimento di Chimica, Biologia e Biotecnologie, Università degli Studi di Perugia, via Elce di Sotto 8, I-06123, Perugia, Italy

^c Dipartimento di Chimica, Biologia e Biotecnologie, Università degli Studi di Perugia, via Elce di Sotto 8, I-06123, Perugia, Italy

^d Dipartimento di Chimica, Fisica e Ambiente, Università di Udine, Via Cottonificio 108, I-33100 Udine, Italy

[‡] These authors equally contributed to the work

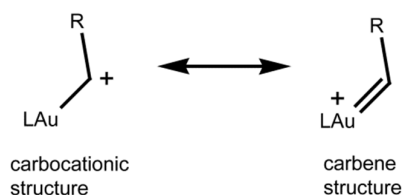
[†] **Electronic Supplementary Information (ESI) available.** Additional tables, figures and DFT-optimized XYZ geometries for all the complexes studied.

Abstract. The geometric perturbation of the cyclopropyl ring in [LAu(S)]ⁿ⁺ (S = cyclopropyl(methoxy)carbene) complexes has been recently proposed as an indirect experimental probe of the [LAu]ⁿ⁺ electron-donating power, but experimental data are available only for a phosphine ligand [Brooner *et al.* Chem. Commun. 2014, 50, 2420, L = P(*t*-Bu)₂(*o*-biphenyl)]. We broaden the study through DFT geometry optimization of a large number of systems, including anionic, neutral and cationic ligands. We combine these results with the accurate calculation, through Charge Displacement analysis, of the Dewar-Chatt-Duncanson components of the Au-carbene bond. The results demonstrate a linear correlation between the distortion of the cyclopropyl ring (Δd) and the Au \rightarrow C π back-donation, which enables to confidently estimate back-donation from a simple geometry optimization or, when available, from experimental data such as X-ray crystal structures. Consequently, Δd can be reliably used to quantitatively determine the position of each system in the *continuum* between the carbocationic and carbene extremes and the percentage of back-donation that S is able to accept (P_{back}). In particular, P_{back} results to be vanishing with cationic ligands, between 18 and 27% with neutral phosphines and carbenes and around 50% with anionic ligands.

Finally, we study the effect of the heteroatom on the substrate, showing that the absolute value of the back-donation is enhanced by around 25% when the methoxy is substituted by a methyl group. Despite of this, since the absence of the heteroatom enhances also the maximum capacity of the carbene to accept back-donation, the position of the systems in the *continuum* is only slightly moved toward the carbene end.

Introduction

In recent years, the use of gold complexes as catalysts for the functionalization of unsaturated carbon-carbon bonds has been growing continuously,¹ inducing many researchers to investigate the nature of the intermediates of the catalytic cycle.² In some cases, such intermediates can be described by two limit resonance structures (Scheme 1), the carbene and carbocation ones,³ which differ essentially for the amount of the Au \rightarrow C back-donation, as defined in the Dewar-Chatt-Duncanson (DCD) model.⁴



Scheme 1. Limit resonance structures of an archetypical intermediate in a $[LAu]^+$ -catalyzed CC functionalization.

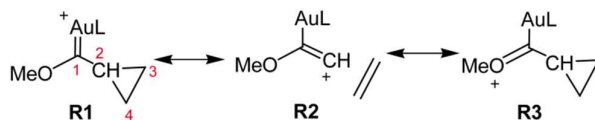
Fürstner and co-workers modeled a typical catalytic intermediate with 1,3-dioxane-2-ethylidene- and 3,3-dimethoxy-propyl-gold species and measured the C_2C_3 rotational barrier.⁵ The resulting low values are consistent with a situation that is better described by the carbocation structure, even if the importance of the latter may have been emphasized by the presence of two carbocation-stabilizing oxygen atoms in the substrate.⁶ Recently, Hashmi, Kästner and coworkers have supported the Fürstner's findings showing that the amount of back-donation (evaluated through the Intrinsic Bond Orbital approach) in relevant gold complexes is generally low.⁷ On the other hand, Toste and co-workers, studying the same rotational barriers by DFT calculations, concluded that actually "the reactivity in gold(I)-coordinated carbenes is best accounted for by a *continuum* ranging from a metal-stabilized singlet carbene to a metal-coordinated carbocation".⁸

New insight into the nature of these key gold species may arise from the synthesis and characterization of non-heteroatom-stabilized gold-carbene complexes, which unfortunately is not

straightforward. Recently, both Straub's and Widenhoefer's groups succeeded in this task with different molecular systems,⁹ evidencing the presence of a certain degree of back-donation.

It is important to underline that the nature of the gold(I)-coordinated intermediates may strongly depend on the ancillary ligands, and systematic work is crucial to establish a scale for the gold-carbon bond nature. The dependence of the DCD components on the ligand, computed through Charge Displacement (CD) analysis,¹⁰ has been determined in a series of recent works by some of us, demonstrating that they can be related to suitably chosen experimental observables.¹¹ In particular, we recently synthesized a series of ten $[\text{LAu-NAC}]^{0/+}$ complexes, having a pyrrolidine moiety bound to the carbenic carbon. We demonstrated that the rotational barrier of the pyrrolidine, measured by NMR spectroscopy, linearly correlates with the $\text{Au} \rightarrow \text{C}$ back-donation, allowing the electronic characterization of different $[\text{LAu}]^{0/+}$ fragments by experimental techniques.¹²

A recent contribution to the debate around the carbocationic/carbene nature of Au-C bond^{13,14,15} has come from a work by Brooner and Widenhoefer, which reported the synthesis and the X-ray crystal structure of a gold cyclopropyl(methoxy)carbene complex $[(\text{JP})\text{AuS}]^+ \text{SbF}_6^-$ [$\text{JP} = \text{P}(t\text{-Bu})_2(o\text{-biphenyl})$, $\text{S} = \text{C}(\text{OMe})(c\text{-Pr})$].¹⁶



Scheme 2. Three limit resonance structures describing the complex $[\text{LAu-S}]^{n+}$ and numbering of the carbon atoms of **S**.

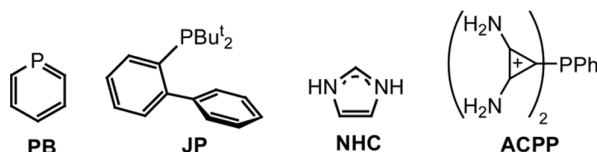
According to previous theoretical work,¹⁷ they related the distortion of a cyclopropyl ring with the electron density at the C_1 , assuming that the electronic structure of $[(\text{JP})\text{AuS}]^+$ can be seen as a combination of the Valence Bond (VB) limit resonance structures **R1-3** (Scheme 2). In particular, **R2** can be seen as an ethene moiety “coordinated” to a cationic methylene unit, as in the original interpretation of Walsh.¹⁸ Therefore, the importance of **R2** can be evaluated by the length of the bonds of the cyclopropyl ring. Such asymmetry can be evaluated by the parameter Δd (Eq. 1)

$$\Delta d = 0.5 * (d_{\text{C}2\text{C}3} + d_{\text{C}2\text{C}4}) - d_{\text{C}3\text{C}4} \quad \text{Eq. 1}$$

Widenhoefer and Brooner compared the Δd of $[(\text{JP})\text{AuS}]^+$ with those of other molecules containing a cyclopropyl moiety bound to π -acceptor groups reported in literature,^{19,20} concluding that the $[(\text{JP})\text{Au}]^+$ fragment donates as much electronic density to C_1 as a cyclopropyl group. Noteworthy,

the carbene moiety chosen by the authors contains only one oxygen atom, which is supposed to provide enough stability to the system without obscuring the effect of gold. To the best of our knowledge, no experimental data for different ligands are available, even though a systematic study would be greatly informative.

For this reason, in this work we have investigated a series of complexes with the general formula of $[LAu-S]^{n+}$ ($n = 0, 1$ or 3), using either anionic [CH_3O^- , Cl^- , F^- , phenyl $^-$ (**Ph**)], cationic (bis[(diamino)cyclo-propenium]phenylphosphines, **ACPP**)²¹ and neutral ligands [**JP**, PPh_3 , pyridine (**Py**), phosphinine (**PB**), carbenes...] (Scheme 3). We selected the ligands for their very different electronic properties, with the aim to widely change the electronic density of the $[LAu]^{n+}$ fragment and study the effects of such change on the experimental properties (geometry and C_1C_2 rotational barrier) of the cyclopropyl ring. For systems possessing the proper symmetry, the donation and back-donation components between $[LAu]^{n+}$ and **S** have been measured decomposing the charge-displacement function (CDF) in contributions from different irreducible representations related to the DCD components.²²



Scheme 3. Structures and abbreviations of some of the ligands considered in this work.

We believe that the results detailed below provide new solid insight into the nature of the Au-C bond and a valuable quantitative model.

Results and Discussion

C_s -symmetric gold(I) complexes. All the $[LAuS]^{n+}$ complexes, if optimized by DFT methods (BP86/TZ2P/ZORA level, see Computational Details) without any constraints, have a similar geometry, with the cyclopropyl moiety perpendicular to the plane containing C_1 , C_2 and O, and the methoxy group lying on the same plane. Such a geometrical arrangement well resembles the solid-state structure of $[(\mathbf{JP})AuS]^+$.¹⁶

If L contains at least one symmetry plane, the whole complex can be conveniently constrained to C_s symmetry, using the carbene plane as the symmetry plane, without any significant change of the geometrical parameters of **S**. In fact, the $d_{C_1C_2}$ and Δd parameters derived from constrained and unconstrained optimizations are practically identical (see Figure S1[†]). These two geometrical parameters turn out to be markedly influenced by L and their variations accurately correlate linearly ($r^2 = 0.9978$, Figure 1), confirming the goodness of the previously proposed framework.¹⁶ In

particular, d_{C1C2} ranges between 1.467 and 1.433 Å for the CH_3O^- and CO ligands, respectively, whereas Δd shows the smallest value for CH_3O^- (0.053 Å) and the largest one for CO (0.106 Å) (See Table S1[†]).

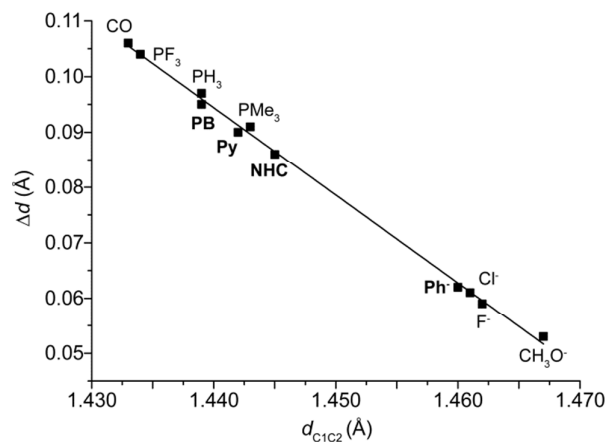


Figure 1. Linear correlation between d_{C1C2} and Δd for $[LAuS]^{+/0}$ complexes.

A qualitative view of the Au-C₁ bond can be obtained by visualizing the electron density difference ($\Delta\rho$) between $[LAuS]^{n+}$ and its fragments ($[LAu]^{n+}$ and **S**), decomposed in two contributions relative to symmetries A' and A''. Considering $[ClAuS]$ as an example (Figure 2), it is possible to see that in the A' symmetry there is a depletion of electronic density at the carbenic carbon, regions of both accumulation and depletion on gold and a remarkable accumulation of electronic density on the chlorine. Since both the carbene lone pair and the unoccupied 6s orbital of gold have A' symmetry, this contribution well describes the **S** → Au σ donation, as recently shown for analogous gold-carbene systems.^{11b}

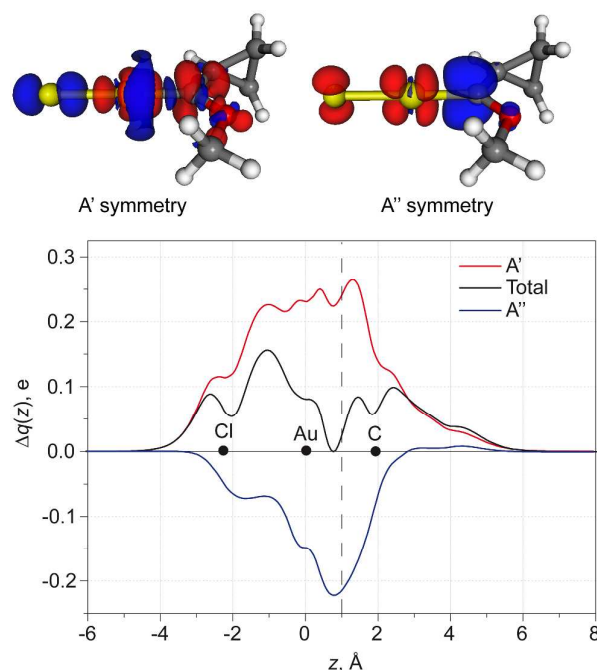


Figure 2. Above: Countour plot of the change of electronic density in A' and A'' symmetry upon formation of the complex [ClAuS]. Blue (red) isosurfaces identify regions in which the electron density increases (decreases). Density value at the isosurfaces: ± 0.0024 au. Bottom: Symmetry-separated Charge Displacement Functions for [ClAuS]. The black dots represent the z coordinate of the atoms. The dotted vertical line identifies a suitable boundary between the two fragments (see text).

On the other hand, the A'' symmetry shows a density depletion on the AuCl fragment and an accumulation on the carbenic carbon. On the latter, the accumulation has the shape of the formally empty p orbital perpendicular to the carbene symmetry plane, while the depletion reflects the shape of the d and p orbitals of gold and chlorine atoms, respectively. The A'' symmetry thus clearly describes the $\text{Au} \rightarrow \text{S} \pi$ back-donation.^{11b} On the substrate, an accumulation of charge is visible on the oxygen: since gold donates electronic density to C₁ upon formation of the bond, the oxygen donates less electrons in the complex than in the case of free S. A similar accumulation, but smaller in magnitude, is present on C₂.

Integrating the two contributions of $\Delta\rho$ along the axis connecting Au and C₁, quantitative information on the charge displacement can be obtained. The two corresponding CDFs for [ClAuS] are shown in the Figure 2 (see also Computational Details). The A' CDF is always positive, denoting an electronic flux from the carbene to the gold fragment (σ donation) that, at the boundary between the fragments (for the definition of the boundary see Computational Details), can be quantified as 0.244 e. On the other hand, the A'' contribution is negative between Au and C₁ (π back-donation)

and it accounts for -0.212 e. The sum of the two components give the net CDF, which is slightly positive at the boundary between Au and C₁ (0.032 e). We mention that these results are only marginally affected by the specific form of the exchange-correlation functional employed in the calculation. The use of different approximations give similar values of the DCD components (Figure S2[†]). In strictly related systems, CD functions are found to be very stable, not only with respect to the exchange-correlation functional,^{11a} but also to the basis set and the level of theory to account the relativistic effects (scalar or full four-component hamiltonian).^{11c}

Interestingly, the DCD components of the bond between AuCl and **NHC** are 0.24 and -0.13 e for the donation and back-donation, respectively.^{11b} While the former is practically the same, the latter is much smaller than in the present case. We explain this by the presence of two nitrogens in **NHC**, which makes C₁ less π acid towards gold.

Expanding our analysis to other C_s-symmetric complexes bearing anionic or neutral ligands, CT_{don} varies from 0.229 to 0.317 e for **Ph**⁻ and PF₃ ligands, respectively. On the other hand, CT_{back} goes from -0.293 to -0.048 e for CH₃O⁻ and CO ligands, respectively, coherently with the high π basicity of the former and the π acidity of the latter.^{11c}

Therefore, in qualitative agreement with the expectations, anionic ligands are associated with large values of CT_{back} , d_{C3C4} and d_{C1C2} (thus favoring structure **R1**, Scheme 2), whereas neutral ligands induce a smaller back-donation and a shortening of the same bonds (structure **R2**, Scheme 1). The C₁O bond distance undergoes a variation that is linearly correlated to d_{C1C2} ($r^2 = 0.9810$, Figure S3[†]), since the oxygen atom can also host the positive charge (structure **R3**, Scheme 2).

With these data in hand, we can quantitatively explore the relationship between the metal-carbon back-donation and the geometric properties of the cyclopropyl moiety. Δd correlates well with both CT_{back} and CT_{tot} ($r^2 = 0.9505$ and 0.9898 , respectively, Figure 3).²³ CT_{don} appears to be almost constant along the series: considering all the systems, the maximum variation of CT_{don} is only 28%, whereas CT_{back} is much more sensitive to the properties of L, with a maximum variation of 82%.

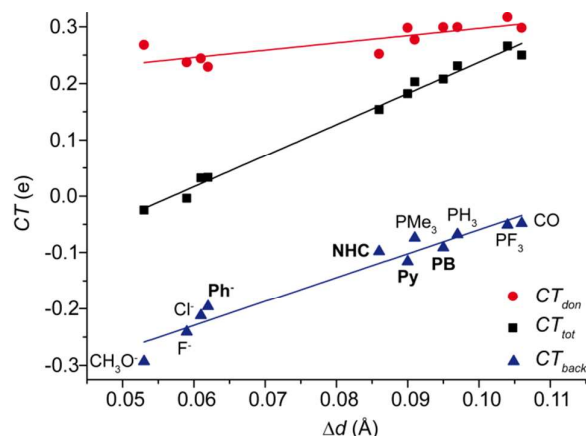


Figure 3. Linear correlations between Δd and CT_{tot} , CT_{don} and CT_{back} for $[\text{LAuS}]^{+0}$ complexes. The fitting equations are: $CT_{\text{tot}} = 5.5\Delta d - 0.31$ ($r^2 = 0.9898$); $CT_{\text{don}} = 1.3\Delta d + 0.17$ ($r^2 = 0.6938$); $CT_{\text{back}} = 4.2\Delta d - 0.48$ ($r^2 = 0.9505$).

It is also interesting to analyze in detail the fitting equation (Eq. 2) relating CT_{back} and Δd .

$$CT_{\text{back}} = 4.2\Delta d - 0.48 \quad \text{Eq. 2}$$

Eq. 2 implies that, when $\Delta d = 0.0$ (the **R1** structure dominates, the back-donation is at its maximum and the Au-C bond can be considered double), CT_{back} is -0.48 e ($CT_{\text{back}}^{\text{max}}$). This value is the maximum back-donation that C_1 is able to accept from gold and it is a measure of the π acidity of **S**. An independent qualitative verification of our model can be found optimizing the geometry of 1-methoxyvinyl-cyclopropane ($\text{H}_2\text{C}=\text{S}^\dagger$), in which the gold fragment is replaced by a methylene unit. Here the CC_1 bond is essentially double (as it actually is in **R1**) and the Δd is quite low, 0.016 Å, as in our model.

Conversely, if the back-donation is null, Δd will be 0.11 Å (Δd_{max} , Eq. 2). This value of Δd is higher than in the case of the free **S** (0.064 Å), and, since there is no back-donation, it has to be due to the combined effect of the polarization of **S** coming from the presence of the metal fragment and the $\text{S} \rightarrow \text{Au}$ σ donation (see ESI for a detailed discussion of this aspect). Actually, the very good linear correlation observed between Δd and CT_{back} is due to the fact that the net effect of polarization and donation does not change dramatically in the series of gold(I) complexes considered here, as reflected by the invariance of CT_{don} . Nevertheless, if systems with a very different value of CT_{don} or different electrostatics are taken into account ($[\text{Cl}_3\text{AuS}]$, $[\text{AuS}]^+$, $[\text{ClAgS}]$ and $[\text{ClCuS}]$), the linear correlation between Δd and CT_{back} is still acceptable ($r^2 = 0.8580$, Figure S6[‡]), while the one between

Δd and CT_{net} becomes poor ($r^2 = 0.7773$). These results confirm that Δd is a robust parameter to estimate the back-donation from experimental information and, in particular, it can be used as a probe of the π donor character of a gold(I)-ligand fragment.

Through Eq. 2, it is now possible to define a parameter that describes for each ligand the amount of $\text{Au} \rightarrow \text{C}_1$ back-donation as the percentage of back-donation (P_{back} , Eq. 3) with respect to the maximum value that C_1 can accept.

$$P_{\text{back}} = 100 * CT_{\text{back}} / CT_{\text{back}}^{\text{max}} = 100 * (\Delta d_{\text{max}} - \Delta d) / \Delta d_{\text{max}} \quad \text{Eq. 3}$$

P_{back} goes from 4 to 52% for $\text{L} = \text{CO}$ and CH_3O^- , respectively (see below and Table S1[†]).

Since Δd and $d_{\text{C}_1\text{C}_2}$ correlate with each other, also the equation relating $d_{\text{C}_1\text{C}_2}$ and CT_{back} can be derived (Eq. 4, Figure S4[†]).

$$CT_{\text{back}} = -6.7d_{\text{C}_1\text{C}_2} + 9.6 \quad \text{Eq. 4}$$

An alternative way to determine the π contribution of a bond is through its rotational barrier.^{5,8,12} In the case of $[\text{LAu-S}]^{+/0}$, the computed rotational barrier ($\Delta^\ddagger E_r$) of the C_1C_2 bond goes from 5.6 to 9.9 kcal/mol for CH_3O^- and CO ligands, respectively (see Table S1 and Figure S5[†]). Such small values indicate that the C_1C_2 bond is in any case more similar to a single bond than to a double bond (low relative importance of structure **R2**). The correlations between $\Delta^\ddagger E_r$ and the Au-S DCD components (Figure S5[†]) are similar to those with Δd (Figure 3), with $r^2 = 0.9582$ and 0.9850 for CT_{back} and CT_{tot} , respectively. The correlation between $\Delta^\ddagger E_r$ and CT_{don} is poor ($r^2 = 0.6513$), as expected. As both Δd and $\Delta^\ddagger E_r$ correlate well with CT_{tot} , there is a very good correlation also between the two observables $\Delta^\ddagger E_r$ and Δd ($r^2 = 0.9922$, Figure S5[†]).

On the other hand, the C_1O rotational barrier is 17.7 and 19.5 kcal/mol for CH_3O^- and CO ligands, respectively, indicating that the structure **R3** is always quite important for the description of the electronic structure of $[\text{LAu-S}]^{0/+}$ complexes. However, the C_1O bond seems to be less sensitive than C_1C_2 to a variation of the $\text{Au} \rightarrow \text{C}_1$ back-donation.

Non-symmetric gold(I) complexes. Since many ligands of catalytic relevance are not C_s -symmetric, such as the phosphines, it is useful to try and extend the analysis to non-symmetric complexes. We consider here different phosphines, such as the ligand used in the Widenhoefer's paper¹⁶ (**JP**) and including aromatic (PPh_3), aliphatic (PCy_3), fluorinated (PAr^{F})²⁴ and cationic (**ACPP**) ones.²¹

Additionally, we study two phosphite ligands, trimethyl- and triphenylphosphite (P(OMe)_3 and P(OPh)_3 , respectively), and a frequently used carbene, **IPr**.

Figure 4a exhibits the correlation between d_{C1C2} and Δd upon inclusion of the non-symmetric systems. The correlation is quite good, with a small deviation for $[\text{JPAu-S}]^+$. This may depend on the steric interference of the ligand on the geometry of **S**. Indeed, **JP** is the only ligand with a protruding moiety toward **S** and this interference is demonstrated by the $\text{AuC}_1\text{C}_2\text{C}_3$ and $\text{AuC}_1\text{C}_2\text{C}_4$ dihedral angles, which are 141.6 and 152.0° , respectively (in all the other complexes the same dihedral angles are very similar to each other and between 145 and 148°).

The correlation between Δd and CT_{tot} is also quite good with non-symmetric species (Figure 4b and Table S3[†]). Moreover, the linear fit function does not change much upon inclusion of the non-symmetric systems, as shown by the comparison of the dashed red line (only symmetric systems) with the continuous black one (all systems).

Since for non-symmetric systems the computation of CT_{back} with the procedure used above is not possible, we took advantage of the Eq. 2 to estimate CT_{back} from Δd . The values obtained are reported in Table 1.

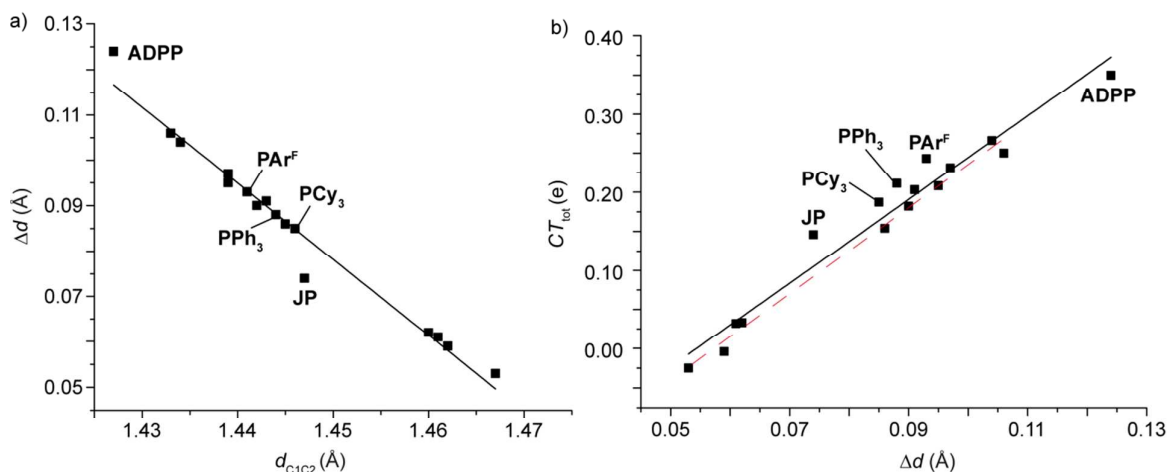


Figure 4. Panel a) Linear correlation between d_{C1C2} and Δd for $[\text{LAuS}]^{n+}$ complexes. Panel b) Linear correlations between Δd and for $[\text{LAuS}]^{n+}$ complexes. The dashed red line refers only to symmetric complexes, whereas the solid black line includes also non-symmetric ones in the fit. The equation of the latter is $CT_{\text{tot}} = 5.4\Delta d - 0.29$ ($r^2 = 0.9563$).

Table 1. Geometrical parameters (in Å) of **S**, computed and estimated Au-C₁ bond properties (in electrons) and P_{back} (%) for non-symmetric $[\text{LAuS}]^{+/0}$ complexes.

L	d_{C1C2}	Δd	CT_{tot}	CT_{back}^a	P_{back}
---	-------------------	------------	-------------------	----------------------	-------------------

JP	1.447	0.074	0.146	-0.134 ^b	26
PPh ₃	1.444	0.088	0.211	-0.110	20
PCy ₃	1.446	0.084	0.187	-0.127	24
PAr^F	1.439	0.094	0.243	-0.085	14
P(OMe) ₃	1.442	0.090	0.203	-0.102	18
P(OPh) ₃	1.441	0.090	0.217	-0.102	18
ACPP	1.427	0.124	0.350	0.041	-12 ^c
IPr	1.450	0.080	0.184	-0.144	27

^a Estimated by Eq. 2, unless otherwise specified.

^b Estimated by Eq. 4. ^c See text.

Remarkably enough, PPh₃ induces a back-donation towards **S** that is only slightly smaller than that induced by PCy₃, whereas the electron-withdrawing **PAr^F** shows a very small CT_{back} , as already seen for the [LAu(NAC)]⁺ and [LAu(C₂H₂)]⁺ complexes.¹² For the cationic phosphine **ACPP**, CT_{back} results to be essentially vanishing (in fact, even slightly positive). This is consistent with the extreme electron-withdrawing power of a dicationic phosphine, which tends to make even the π electrons to flow from **S** to the metal fragment.

For **JP**, as stated before, Δd cannot be used to estimate the corresponding value of CT_{back} , because it is markedly influenced by the steric hindrance of the *o*-biphenyl moiety of the ligand. Since the steric influence is likely much smaller on d_{C1C2} than on Δd , Eq. 4 gives a more reliable value than Eq. 2. The resulting CT_{back} for [JPAu-S]⁺ is -0.134 e, slightly higher than PCy₃ (-0.127 e).

As a consequence of the results shown above, Δd can indeed be used to quantitatively determine the position of each molecular system in the *continuum* going from the Au-C single bond (no back-donation) to the Au=C double bond (maximum back-donation) (Figure 5). As stated earlier, the two extreme ends of the spectrum correspond to a Δd of 0.11 and 0.00 Å, respectively.

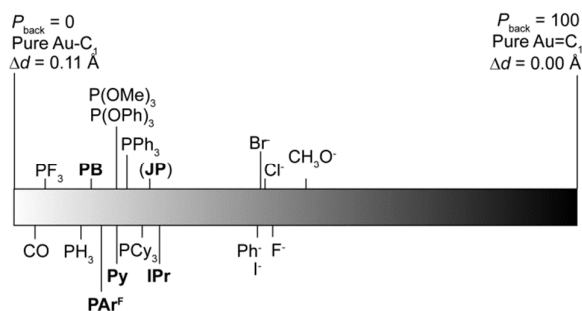
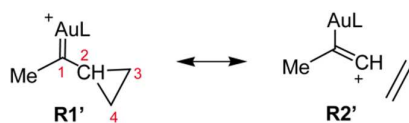


Figure 5. Position of [LAuS]ⁿ⁺ complexes in the *continuum* between single and double AuC₁ bond.

JP is in bracket because it is estimated from Eq. 4 instead of Eq. 2.

The diagram shows very well that almost all the systems are closer to the “carbocation” end of the *continuum*, even if the ancillary ligand can remarkably tune such position. The [OCH₃Au] fragment lies in the middle of the spectrum ($P_{\text{back}} = 52\%$). Notably, all the ligands frequently used in catalysis are quite close to each other, with P_{back} between 18% (phosphite ligand) and 27% (**IPr**). Remarkably, this trend is the same as that emerged from experimental observations,¹² but we have now placed it on solid theoretical ground. In the case of [(**ACPP**)AuS]³⁺, Δd is even higher than 0.11 Å and out of the range of Figure 5 ($CT_{\text{back}} > 0$), but there are no doubts that in this case the Au-C₁ bond is essentially single.

Non-heteroatom-stabilized carbene. It is now interesting to measure the effect of the heteroatom bound to C₁ on the DCD components of the Au-C bond. For this, the methoxy group has been substituted with a simple methyl, obtaining the substrate **S'** and the series of complexes [LAuS']. Since the methyl is not able to host a positive charge, only two VB structures are important: **R1'**, having complete Au → C₁ back-donation (CT'_{back}), and **R2'**, having no Au → C₁ back-donation and a double bond between C₁ and C₂ (Scheme 4). Also in this case the cyclopropyl distortion ($\Delta d'$) should be related to the relative weight of **R1'** and **R2'**.



Scheme 4.

Since the substrate has changed, also the equation relating CT'_{back} and $\Delta d'$ will be different. In order to derive it, four complexes were optimized with L = CO, **NHC**, Cl⁻ and CH₃O⁻, purposely chosen to cover all the range of back-donation. In line with our model, also in this case a linear correlation between the two properties can be found ($r^2 = 0.9763$, Figure S8[†]).

Interestingly, all the $\Delta d'$ values are remarkably larger than the corresponding Δd ones, going from 0.168 to 0.079 Å for L = CO and CH₃O⁻, respectively, an indication that the relative importance of the VB structure **R2'** is larger. Confirming this, $\Delta^{\ddagger}E_r$ for the C₁C₂ bond of [ClAuS'] is 8.7 kcal/mol, which is 2.5 kcal/mol larger than in the case of [ClAuS].²⁵ Also the CT_{back} values are systematically larger than in the case of [LAuS]ⁿ⁺, going from -0.064 to -0.374 e for L = CO and CH₃O⁻, respectively. This means that also **R1'** is more important than before, and this can be easily explained considering that the absence of the heteroatom makes the p_z orbital of C₁ more π acidic.

Consequently, C_1 attracts more electron density from both gold (enhancement of back-donation) and C_2 (enhancement of $\Delta d'$ and $\Delta^\ddagger E_r$).

The fit equation relating CT'_{back} and $\Delta d'$ for $[\text{LAuS}']^{n+}$ is

$$CT'_{\text{back}} = 3.5\Delta d' - 0.63 \quad \text{Eq. 5}$$

According to Eq. 5, the maximum back-donation ($\Delta d' = 0$) that S' can receive from gold is -0.63 e, which is markedly more negative than the value for S (-0.48 e). Conversely, when the back-donation is null, $\Delta d'_{\text{max}}$ results to be 0.18 Å, which is higher than Δd_{max} (0.11 Å). As before, optimizing the geometry of $\text{H}_2\text{C}=\text{S}'$, which simulates a system with a real double bond (maximum back-donation), leads to a very small cyclopropyl distortion ($\Delta d' = 0.019$ Å).

Once again, taking advantage of Eq. 5, the back-donation can be estimated for any non-symmetric ligand, starting from a simple geometrical optimization. For all the ligands CT'_{back} is systematically higher than CT_{back} , and this fact underlines the active role of the heteroatom in the modulation of the back-donation, with an increase around 25% (Figure S9[†]). However, such an increase does not alter the trend of the ligands.

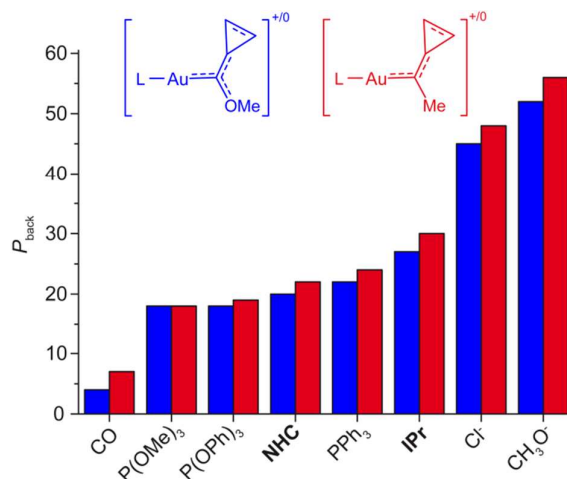


Figure 6. Comparison between the percentage of $\text{Au} \rightarrow C_1$ π back-donation (P_{back}) for $[\text{LAuS}]^{+/0}$ and $[\text{LAuS}']^{+/0}$ in presence of different ligands.

Comparing the P_{back} values for $[\text{LAuS}]^{+/0}$ and $[\text{LAuS}']^{+/0}$ in presence of different ligands (Figure 6), it can be seen that the values are very similar and in some cases within our range of confidence (± 1). However, we note that P_{back} is systematically higher in the case of S' , an indication that the carbene character of the $\text{Au}-C_1$ bond is always slightly stronger without the heteroatom.

Conclusion.

In conclusion, we analyzed the Au-C₁ bond properties of a series of C_s-symmetric [LAu-S]^{0/+} complexes, demonstrating that the electronic properties of L influence both the Dewar-Chatt-Duncanson components of the Au-C₁ bond and the experimental properties of S, such as the C₁C₂ bond length, the cyclopropyl asymmetry (Δd) and the C₁C₂ rotational barrier ($\Delta^\ddagger E_r$). All of them can be directly correlated to the Au \rightarrow C₁ back-donation and to the net charge displacement, in agreement with the two limit resonance structures, the carbene and carbocation ones. The implication of such a correlation is that the back-donation can be accurately estimated by a simple DFT optimization, or, experimentally, either by the analysis of the X-ray crystal structures of the complexes (in principle, at least²⁶) or the measurement of rotational barriers.

Here the correlation has been usefully used to estimate the nature of the Au-C bond for nonsymmetric ligands frequently used in catalysis, for which the CDF cannot be decomposed by symmetry, such as triphenylphosphine. In this way, it has been possible to quantitatively determine the position of each ligand in the *continuum* between the two limit resonance structures (Au-C⁺ and Au⁺=C). These results provide new solid bases to quantitatively estimating the amount of “carbene character” of the Au-C bond.

Our result indicate that the back-donation is null with cationic ligands, below 30% with neutral ligands and around 50% with anionic ligands. Noteworthy, phosphites, phosphines and carbenes induce a variation of few percentage points of P_{back} (18-27% of the maximum back-donation), but the trend is the same qualitatively derived from experimental observations.¹⁴

The effect of the heteroatom has been studied, too, optimizing a series of non-heteroatom-carbene gold complexes [LAuS']^{0/+}, revealing, as expected, an enhanced π acidity of C₁. More importantly, the simple approach presented here allows us to quantify such an enhancement starting from the cyclopropyl asymmetry, showing that the substitution of a methoxy group with a methyl enhances the back-donation by about 25% for all the systems, without altering the trend within the series. Despite this, since also the maximum back-donation increases, the position of the ligands in the spectrum shows a small increase.

Coherently, it is interesting to note that the presence of two nitrogen atoms lowers the Au \rightarrow C₁ back-donation to approximately one half (-0.11 e in the case of [ClAuNAC],¹² -0.13 e in the case of [ClAuNHC]^{11b}) with respect to [ClAuS], but, again, the trend of the ligands is always the same and irrespective of the substrate used as a probe.

Now that quantitative and unambiguous information are available, it would be important to connect our results with the catalytic examples in which a difference of the Au \rightarrow C₁ back-donation has been

invoked to explain the ligand effect in catalysis.^{13,14} Indeed, the difference between phosphines and carbenes seems to be moderate in terms of CT_{back} (Figure 5), but even a “small” difference could have a large impact on the catalytic output. Similarly, the synthesis of new charged ligands, such as the cationic **ACPP**, could be interesting to explore the effect of large variations of back-donation on catalytic performance. Further research on these matters is currently underway in our laboratory.

Computational details

All calculations were carried out using density functional theory employing the BP86²⁷ functional as implemented in the ADF package (v.2009).^{28,29,30} A triple zeta basis set with two polarization functions was used on all atoms (TZ2P) with a small frozen core.²⁸ Relativistic effects were included by means of zeroth-order regular approximation (ZORA) Hamiltonian.^{31,32,33} According to our recent benchmark, the BP86 functional revealed to be very reliable for geometry optimizations (average mean error with respect to Coupled Cluster-optimized geometry smaller than 1 pm).³⁴ The changes in electron density encountered upon bond formation were analysed by means of the charge-displacement (CD) function (Eq. 6):

$$\Delta q(z) = \int_{-\infty}^{\infty} dx \int_{-\infty}^{\infty} dy \int_{-\infty}^z dz' \Delta \rho(x, y, z') \quad \text{Eq. 6}$$

where $\Delta \rho(x, y, z)$ is the difference between the electron densities of a complex and the sum of that of its non-interacting fragments, frozen at the same geometry they assume in the complex. $\Delta q(z)$ defines at each point z along a chosen axis the amount of electron charge that moves through a plane perpendicular to the given axis through z . Accordingly, a positive slope describes regions of charge accumulation whilst a negative slope denotes charge depletion.

In order to quantify the charge transfers (CT) upon the coordination of **S** (or **S'**) on $[\text{LAu}]^{n+}$, it is useful to fix a plausible boundary separating the fragments in the complexes. We choose the isodensity value representing the point on the z axis at which equal-valued isodensity surfaces of the isolated fragments are tangent.²²

For C_s symmetry-constrained systems, the chosen symmetry plane is that containing C_1 , C_2 and O , with the z axis passing through the M-C bond. This allows the separation of the net charge displacement $\Delta \rho$ into the contributing components, according to Eq. 7 and 8:

$$\Delta \rho = \sum_p \Delta \rho_p \quad \text{Eq. 7}$$

$$\Delta\rho_p = \sum_{i \in p} |\phi_i^{(AB)}|^2 - \sum_{i \in p} |\phi_i^{(A)}|^2 - \sum_{i \in p} |\phi_i^{(B)}|^2 \quad \text{Eq. 8}$$

where p labels the irreducible representation A' and A''. AB, A and B represent the complex of the two fragments and the two separate fragments, respectively, while ϕ_i are the Kohn-Sham orbitals. A symmetry-independent methodology to separate the DCD components has been recently published.³⁵ For the geometry optimizations and the frequency calculations in presence of point charges we used a fine integration grid (6), the keyword "Branch Old" and we set the value of the "qpnear" keywords to 20.

Acknowledgements

This work was supported by grants from the Ministero dell'Istruzione dell'Universita e della Ricerca (MIUR) through FIRB-futuro in ricerca (RBF1022UQ, Novel Au(I)-based molecular catalysts: from know-how to know-why, "AuCat").

Corresponding authors

*Email: leonardo.belpassi@cnr.it; ggiancaleoni@gmail.com

References

- ¹ S. M. Inamdar, A. Konala, N. T. Patil, *Chem. Commun.* 2014, **50**, 15124-15135; L. Fensterbank, M. Malacria, *Acc. Chem. Res.* 2014, **47**, 953-965; A. S. K. Hashmi, *Acc. Chem. Res.* 2014, **47**, 864-876; M. Rudolph, A. S. K. Hashmi, *Chem. Soc. Rev.* 2012, **41**, 2448-2462; M. Bandini, *ACS Cat.* 2015, **5**, 1638-1652; D. J. Gorin, F. D. Toste, *Nature* 2007, **446**, 395-403; A. Fürstner, P. W. Davies, *Angew. Chem. Int. Ed.* 2007, **46**, 3410-3449;
- ² T. Lauterbach, A. M. Asiri, A. S. K. Hashmi, *Adv. Organomet. Chem.* 2014, **62**, 261-297; R. E. M. Brooner, R. A. Widenhoefer, *Angew. Chem. Int. Ed.* 2013, **52**, 11714-11724; L. Liu, G. B. Hammond, *Chem. Soc. Rev.* 2012, **41**, 3129-3139; D. Zuccaccia, L. Belpassi, F. Tarantelli, A. Macchioni, *Eur. J. Inorg. Chem.* 2013, **24**, 4121-4135; C. Obradors, A. M. Echavarren, *Chem. Commun.* 2014, **50**, 16-28.
- ³ A. S. K. Hashmi, *Angew. Chem. Int. Ed.* 2008, **47**, 6754-6756; A. M. Echavarren, *Nature Chem.* 2009, **1**, 431-433.
- ⁴ M. J. S. Dewar, *Bull. Soc. Chim. Fr.*, 1951, C71-C9; J. Chatt, L. A. Duncanson, *J. Chem. Soc.* 1953, 2939-2947.
- ⁵ G. Seidel, R. Mynott, A. Fürstner, *Angew. Chem. Int. Ed.* 2009, **48**, 2510-2513.
- ⁶ M. M. Hansmann, F. Rominger, A. S. K. Hashmi, *Chem. Sci.* 2013, **4**, 1552-1559.
- ⁷ L. N. d. S. Comprido, J. E. M. N. Klein, G. Knizia, J. Kästner, A. S. K. Hashmi, *Angew. Chem. Int. Ed.* DOI: 10.1002/anie.201412401.
- ⁸ D. Benitez, N. D. Shapiro, E. Tkatchouk, Y. Wang, W. A. Goddard, F. D. Toste, *Nat. Chem.* 2009, **1**, 482-486.
- ⁹ M. W. Hussong, F. Rominger, P. Krämer, B. F. Straub, *Angew. Chem. Int. Ed.* 2014, **53**, 9372-9375; R. J. Harris, R. A. Widenhoefer, *Angew. Chem.* 2014, **126**, 9523-9525.
- ¹⁰ L. Belpassi, I. Infante, F. Tarantelli, L. Visscher, *J. Am. Chem. Soc.* 2008, **130**, 1048-1060.

- ¹¹ (a) G. Bistoni, F. Tarantelli, L. Belpassi, *Angew. Chem. Int. Ed.* 2013, **52**, 11599-11602; (b) D. Marchione, L. Belpassi, G. Bistoni, A. Macchioni, F. Tarantelli, D. Zuccaccia, *Organometallics* 2014, **33**, 4200-4208; (c) G. Ciancaleoni, N. Scafuri, G. Bistoni, A. Macchioni, F. Tarantelli, D. Zuccaccia, L. Belpassi, *Inorg. Chem.* 2014, **53**, 9907-9916.
- ¹² G. Ciancaleoni, L. Biasiolo, G. Bistoni, A. Macchioni, F. Tarantelli, D. Zuccaccia, L. Belpassi, *Chem. – Eur. J.* 2015, **21**, 2467-2473.
- ¹³ Y. Xi, Y. Su, Z. Yu, B. Dong, E. J. McClain, Y. Lan, X. Shi, *Angew. Chem. Int. Ed.* 2014, **53**, 9817-9821; G. Seidel, B. Gabor, R. Goddard, B. Heggen, W. Thiel, A. Fürstner, *Angew. Chem. Int. Ed.* 2014, **53**, 879-882; R. Döpp, C. Lothschütz, T. Wurm, M. Pernpointner, S. Keller, F. Rominger, A. S. K. Hashmi, *Organometallics* 2011, **30**, 5894-5903; G. Seidel, A. Fürstner, *Angew. Chem. Int. Ed.* 2014, **53**, 4807-4811; M. Alcarazo, T. Stork, A. Anoop, W. Thiel, A. Fürstner, *Angew. Chem. Int. Ed.* 2010, **49**, 2542-2546; A. Fürstner, L. Morency, *Angew. Chem. Int. Ed.* 2008, **47**, 5030-5033.
- ¹⁴ Y. Wang, M. E. Muratore, A. M. Echavarren, *Chem. Eur. J.* 2015, **21**, 7332-7339.
- ¹⁵ R. J. Harris, R. A. Widenhoefer, *Angew. Chem. Int. Ed.* 2015, **54**, 6867-6869.
- ¹⁶ R. E. M. Brooner, R. A. Widenhoefer, *Chem. Commun.* 2014, **50**, 2420-2423.
- ¹⁷ T. Clark, G. W. Spitznagel, R. Klose, P. v. R. Schleyer, *J. Am. Chem. Soc.* 1984, **106**, 4412-4419; R. Hoffmann, *Tetrahedron Lett.* 1970, **11**, 2907-2909; H. Günther, *Tetrahedron Lett.* 1970, **11**, 5173-5176; R. Hoffmann, R. B. Davidson, *J. Am. Chem. Soc.* 1971, **93**, 5699-5705.
- ¹⁸ A. D. Walsh, *Nature* 1947, **159**, 165; A. D. Walsh, *Trans. Faraday Soc.* 1949, **45**, 179-190.
- ¹⁹ F. H. Allen, *Acta Crystallogr., Sect. B* 1980, **36**, 81-96; F. H. Allen, *Acta Crystallogr., Sect. B* 1981, **37**, 890-900.
- ²⁰ G. A. Olah, V. P. Reddy, G. K. S. Prakash, *Chem. Rev.* 1992, **92**, 69-95.
- ²¹ J. Carreras, G. Gopakumar, L. Gu, A. Gimeno, P. Linowski, J. Petušková, W. Thiel, M. Alcarazo, *J. Am. Chem. Soc.* 2013, **135**, 18815-18823.
- ²² N. Salvi, L. Belpassi, F. Tarantelli, *Chem. Eur. J.* 2010, **16**, 7231-7240.
- ²³ Similar correlations can be found between the components of *CT* and d_{C1C2} (Figure S3†).
- ²⁴ D. Zuccaccia, L. Belpassi, L. Rocchigiani, F. Tarantelli, A. Macchioni, *Inorg. Chem.* 2010, **49**, 3080-3082; L. Biasiolo, L. Belpassi, G. Ciancaleoni, A. Macchioni, F. Tarantelli, D. Zuccaccia, *Polyhedron* 2015, **92**, 52-59.
- ²⁵ Toste and coworkers observed a similar effect on different systems, see ref. 7.
- ²⁶ According to our optimized geometries, the effect of the back-donation on Δd could be too small to be actually revealed by X-ray crystallography.
- ²⁷ A. D. Becke, *Phys. Rev. A* 1988, **38**, 3098-3100; J. P. Perdew *Phys. Rev. B* 1986, **33**, 8822-8824.
- ²⁸ ADF Users Guide. Release 2008.1, SCM, Theoretical Chemistry, Vrije Universiteit, Amsterdam, 2008, <http://www.scm.com>.
- ²⁹ C. Fonseca Guerra, J. G. Snijders, G. Te Velde, E. J. Baerends, *Theor. Chem. Acc.* 1998, **99**, 391-403.
- ³⁰ G. Te Velde, F. M. Bickelhaupt, E. J. Baerends, C. Fonseca Guerra, S. J. A. van Gisbergen, J. G. Snijders, T. Ziegler, *J. Comput. Chem.* 2001, **22**, 931-967.
- ³¹ E. van Lenthe, E. J. Baerends, J. G. Snijders, *J. Chem. Phys.* 1993, **99**, 4597-4610.
- ³² van Lenthe, E.; Baerends, E. J.; Snijders, J. G. *J. Chem. Phys.* 1994, **101**, 9783-9792.
- ³³ van Lenthe, E.; Ehlers, A.; Baerends, E. J. *J. Chem. Phys.* 1999, **110**, 8943-8953.
- ³⁴ G. Ciancaleoni, S. Rampino, D. Zuccaccia, F. Tarantelli, P. Belanzoni, L. Belpassi, *J. Chem. Theory Comput.*, 2014, **10**, 1021-1034.
- ³⁵ G. Bistoni, S. Rampino, F. Tarantelli, L. Belpassi, *J. Chem. Phys.*, 2015, **142**, 084112.

TABLE OF CONTENT

Synopsis. A simple geometrical parameter can be used to easily evaluate the Au \rightarrow C₁ backdonation.

